Observation and Quadrupole-Moment Measurement of the First Superdeformed Band in the $A \sim 60$ Mass Region

C. E. Svensson,[1] C. Baktash,[2] J. A. Cameron,[1] M. Devlin,[3] J. Eberth,[4] S. Flibotte,[1] D. S. Haslip,[1] D. R. LaFosse,[3] I. Y. Lee,[5] A. O. Macchiavelli,[5] R. W. MacLeod,[5] J. M. Nieminen,[1] S. D. Paul,[2] L. L. Riedinger,[6] D. Rudolph,[7] D. G. Sarantites,[3] H. G. Thomas,[4] J. C. Waddington,[1] W. Weintraub,[6] J. N. Wilson,[1] A. V. Afanasjev,[8,*] and I. Ragnarsson[8]

[1]*Department of Physics and Astronomy, McMaster University, Hamilton, Ontario, Canada, L8S 4M1*
[2]*Physics Division, Oak Ridge National Laboratory, Oak Ridge, Tennessee 37831-6371*
[3]*Chemistry Department, Washington University, St. Louis, Missouri 63130*
[4]*Institut für Kernphysik, Universität zu Köln, D-50937 Köln, Germany*
[5]*Nuclear Science Division, Lawrence Berkeley Laboratory, Berkeley, California 94720*
[6]*Department of Physics and Astronomy, University of Tennessee, Knoxville, Tennessee 37996*
[7]*Sektion Physik, Ludwig-Maximilians-Universität München, D-85748 Garching, Germany*
[8]*Department of Mathematical Physics, Lund Institute of Technology, S-22100 Lund, Sweden*

(Received 6 May 1997)

A high-spin rotational cascade of six γ rays has been observed in ^{62}Zn. The quadrupole moment of $2.7^{+0.7}_{-0.5}$ e b measured for this band corresponds to a deformation $\beta_2 = 0.45^{+0.10}_{-0.07}$. The properties of this band are in excellent agreement with calculations that predict high-spin superdeformed bands in ^{62}Zn with deformations $\beta_2 = 0.41-0.49$. These results establish a new region of superdeformation for nuclei with neutron and proton numbers $N, Z \approx 30-32$. [S0031-9007(97)03901-X]

PACS numbers: 21.10.Re, 21.10.Ky, 23.20.Lv, 27.50.+e

In recent years the study of superdeformed (SD) bands has been one of the most exciting topics in nuclear structure research. Since the first observation of high-spin superdeformation in ^{152}Dy [1], SD bands have been identified in many nuclei in the $A \sim 190, \sim 150, \sim 130$, and ~ 80 mass regions [2]. Based on calculations of large SD shell gaps in the single-particle energy levels for particle numbers $N, Z \approx 30-32$ [3,4], SD bands have also been predicted in the $A \sim 60$ mass region [5]. Because of the limited number of particles in these nuclei and their proximity to the $N = Z$ line, superdeformation in this mass region is of particular interest. Studies of $A \sim 60$ SD bands will enable comparisons between mean-field cranking models of SD nuclei and large-scale shell model calculations [6], studies of the onset of isospin $T = 0$ neutron-proton pairing at high rotational frequency [7,8], and investigations of the loss of collectivity in these SD bands resulting from the limited spin content of their single-particle configurations [9]. However, because of a number of experimental difficulties, previous searches for these bands have been unsuccessful. In this Letter we report on the observation of a SD band in ^{62}Zn, the first observation of $A \sim 60$ superdeformation.

High-spin states in ^{62}Zn were populated via the ^{40}Ca(^{28}Si, $\alpha 2p$)^{62}Zn reaction at a bombarding energy of 125 MeV. A thin (500 μg/cm^2) target enriched to 99.9% in ^{40}Ca was used, and the detection system consisted of the Gammasphere array [10] comprising 83 Compton-suppressed Ge detectors, 15 neutron detectors, and the Microball [11], a 4π charged-particle detector array consisting of 95 CsI(Tl) scintillators. The collimators were removed from the Ge detectors, allowing γ-ray multiplicity and sum-energy information to be measured for each event [12]. With an event trigger requiring coincidences between at least three Ge detectors or between at least two Ge detectors and a neutron detector, 2.7×10^9 events were recorded in five days of beam time. The $\alpha 2p$ evaporation channel leading to ^{62}Zn comprised $\sim 10\%$ of the total fusion cross section in this reaction and was selected by applying the total energy plane channel-selection method [13] to events in which an alpha particle and two protons were detected in the Microball. Events passing the selection criteria were unpacked into a symmetrized $E_\gamma - E_\gamma$ correlation matrix which contained 5.0×10^8 γ-γ coincidences, 95% of which were associated with ^{62}Zn.

In addition to the normally deformed (ND) bands in ^{62}Zn identified in an earlier experiment [14], a new band consisting of a cascade of six γ rays was observed. Figure 1 shows the γ spectrum obtained by summing coincidence gates set on all of the members of this band. The γ-ray energies, which have uncertainties of ± 2 keV, are labeled in this figure. Also labeled are the energies of known transitions in ^{62}Zn which firmly establish the new band as belonging to this nucleus. The observed intensity of the band in the plateau region was $\sim 1\%$ of the channel intensity, as shown in the inset of Fig. 1(a). Although the band was weakly populated, single gates were sufficiently clean to confirm the mutual coincidence of all of the γ rays except the 1993 keV transition. This transition was confirmed as a member of the band by summing double gates set on the band members in an $E_\gamma - E_\gamma - E_\gamma$ coincidence cube. The stretched $E2$ character of the γ rays was confirmed by their angular distributions.

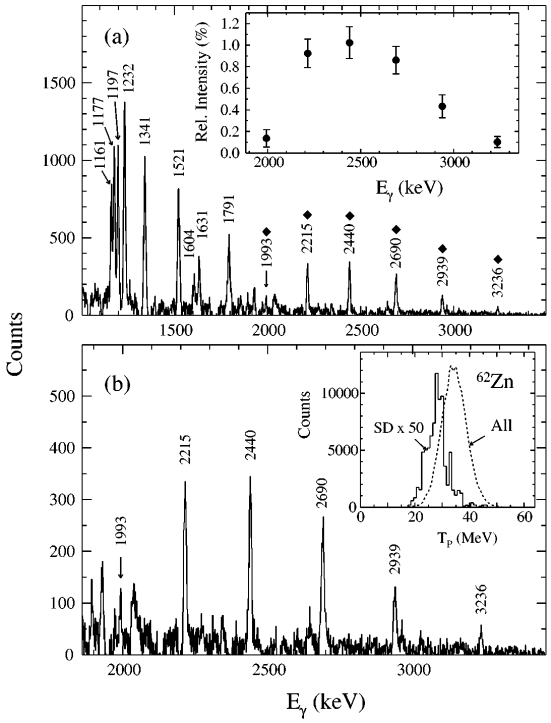

FIG. 1. γ-ray spectrum generated by summing coincidence gates set on all of the transitions in the new band (diamonds). (a) Energies label the band members and known transitions in ^{62}Zn; (b) expanded view of the band. The inset in (a) shows the intensity of the band relative to the channel. The inset in (b) shows spectra of the sum of the particle kinetic energies T_p in the center of mass frame for the band (solid line) and the $\alpha 2p$ channel (dashed line) obtained by triple gating on γ rays from the band and from low-spin states in ^{62}Zn, respectively.

Although a 3986 keV γ ray was observed in coincidence with the band and appears to be a decay-out transition, the lack of statistics prevented a conclusive linking of this band into the ^{62}Zn decay scheme. The 3986 keV γ ray carries only $\sim 8\%$ of the intensity of the band and the remainder of the decay-out intensity is highly fragmented, as is typical of the decay out of SD bands in other mass regions (e.g., [15]). Although the band is not linked into the decay scheme, its high-spin nature is revealed by its decay into known high-spin states. The 1161 and 1791 keV γ rays in Fig. 1(a), for example, arise from states with $I^\pi = 14^+$ and 13^-, respectively [14]. In addition, the excitation energy at which the band is fed can be accurately determined by measuring the sum of the particle kinetic energies T_p in the center of mass frame [16]. The inset in Fig. 1(b) shows T_p spectra in coincidence with the band (solid line) and low-spin states in ^{62}Zn (dashed line). The mean T_p of 28.8 MeV for events feeding the band is 6.2 MeV below the average for the $\alpha 2p$ channel. The corresponding mean total γ-ray energy of 32.0 MeV for decays that pass through the band is thus 6.2 MeV larger than the ^{62}Zn average. These spectra show that the band is populated by only the highest excitation energy, and hence highest spin, components of the ^{62}Zn entry distribution. Based on the decay of the band into known high-spin states, a decay-out energy of at least 3986 keV, the excitation energy at which the band is fed, its intensity profile, and calculations (see below) which predict that the SD bands in ^{62}Zn become yrast for spins $I \geq 24\hbar$, we estimate that the observed band extends from $I = 18\hbar$ to $30\hbar$ with a $\pm 2\hbar$ uncertainty.

In Fig. 2 we plot the dynamical moment of inertia $J^{(2)}$ as a function of rotational frequency for the new band and for typical SD bands from the other regions of superdeformation. In order to remove the mass dependence, all of the $J^{(2)}$ values have been divided by $A^{5/3}$ [17]. The scaled $J^{(2)}$ values for the ^{62}Zn band are comparable to those for SD bands in other mass regions, and we note that the ^{62}Zn band extends to the highest rotational frequency observed for a SD band.

Although the large moment of inertia of the new band, its intensity profile, its feeding from the highest-spin components of the entry distribution, and its fragmented decay out into known high-spin states all support a SD interpretation, a definitive conclusion on the deformation of this band requires a measurement of its transition quadrupole moment Q_t. Because of the high collectivity and high transition energies of this band, the state lifetimes (on the order of 1 fs) are much shorter than the time taken by the recoiling nucleus to leave the target (on the order of 100 fs). The entire band thus decays while the nucleus is slowing down in the target and Q_t can be measured by the thin target Doppler shift attenuation method [18]. The measured fraction F of the full Doppler shift is plotted versus γ-ray energy for a number of transitions in Fig. 3. Most of the transitions from states with $I \leq 14\hbar$ decay outside of the target with constant shift $F = 0.872$, the ND bands in ^{62}Zn decay on the same time scale as the time to recoil out of the target, and all of the transitions in the new band have very short lifetimes and are almost fully shifted.

In order to extract the quadrupole moment of the new band, the slowing down of the recoiling nuclei in the target was modeled using the electronic stopping powers

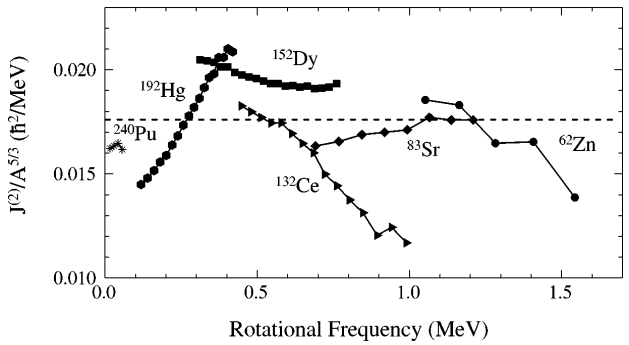

FIG. 2. Plot of the dynamical moment of inertia $J^{(2)}$ divided by $A^{5/3}$ versus rotational frequency for the new band in ^{62}Zn and for SD bands from other mass regions. For reference, the dashed line represents the moment of inertia of a rigid rotor with quadrupole deformation $\beta_2 = 0.5$.

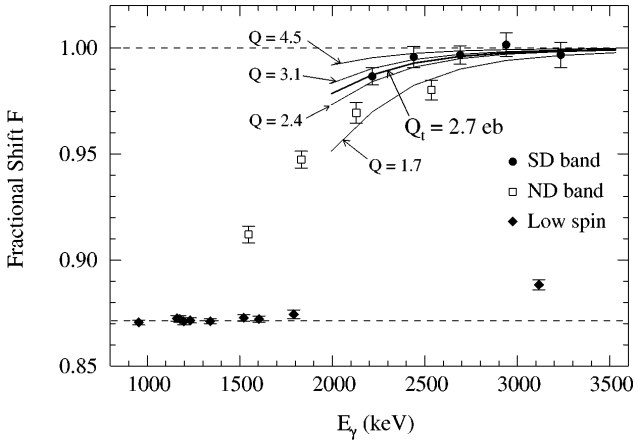

FIG. 3. Fractional Doppler shifts F for transitions from states with $I \leq 14\hbar$ (diamonds), for a ND band in ^{62}Zn (squares), and for the new band (circles). The dashed lines at $F = 1.00$ and 0.872 represent the full shift and the constant shift for decays outside of the thin target, respectively. Calculated F curves for various Q_t values are shown by solid lines. The new band is best fit by $Q_t = 2.7^{+0.4}_{-0.3}\ e$ b.

of Northcliffe and Schilling [19] scaled by the Ziegler and Chu [20] stopping powers for ^{4}He as suggested by Sie *et al.* [21]. The mean velocity of the recoiling nuclei was calculated as a function of time by integrating over the target and averaging over 100 reaction locations within the target. The decay of the nucleus was modeled by assuming a constant in-band Q_t, and side feeding into each state was modeled by a single transition with the same lifetime as the precursor in-band state [22] and an intensity to match the observed intensity profile of the band. The fractional shifts calculated in this model for various Q_t values are shown by solid curves in Fig. 3. The new band is best fit by $Q_t = 2.7^{+0.4}_{-0.3}\ e$ b. Investigations of various decay models revealed that the uncertainty associated with the side feeding was insignificant in comparison with the uncertainty associated with the modeling of the slowing-down process which, when combined with the above statistical uncertainty, yields a Q_t value of $2.7^{+0.7}_{-0.5}\ e$ b for the band. Assuming an axially symmetric shape, the corresponding quadrupole deformation is $\beta_2 = 0.45^{+0.10}_{-0.07}$.

We have carried out a theoretical analysis of high-spin states in ^{62}Zn employing the configuration-dependent shell-correction approach with the cranked Nilsson potential [23,24]. Representative potential energy surfaces calculated for $I^\pi = 20^-$ and 24^- are shown in Figs. 4(a) and 4(b), respectively, and the energies of favored high-spin collective configurations are plotted versus spin in Fig. 4(c). At moderate spins the yrast configurations are triaxial signature-degenerate ND bands ($\beta_2 \approx 0.3, \gamma \approx 30°$) which approach the $\gamma = 60°$ noncollective axis at higher spins. These correspond to the smoothly terminating strongly coupled bands previously observed [14] in ^{62}Zn. For higher spins ($I \geq 24\hbar$) the yrast configurations are calculated to be SD bands with deformations $\varepsilon_2 = 0.36$–0.43 ($\beta_2 = 0.41$–0.49), $\gamma = 0°$–$15°$.

In all of the favored SD bands the neutron and proton orbitals up to the $N, Z = 30$ SD shell gap corresponding to the $f_{7/2}$-hole $g_{9/2}$-particle configuration $[f_{7/2}]^{-2}[g_{9/2}]^2$ are filled. Different SD bands are formed depending on the orbitals occupied by the last two neutrons. The observed band in ^{62}Zn is assigned to one of the neutron SD configurations $\nu[f_{7/2}]^{-2}[g_{9/2}]^{2,3}$. The Q_t values calculated (as in [9]) for these bands in the spin range of interest, namely, $Q_t = 2.7$–$2.1\ e$ b for the $\nu[f_{7/2}]^{-2}[g_{9/2}]^2$ configuration and $Q_t = 3.2$–$2.5\ e$ b for the $\nu[f_{7/2}]^{-2}[g_{9/2}]^3$ configurations agree well with the measured value of $2.7^{+0.7}_{-0.5}\ e$ b. The $\nu[f_{7/2}]^{-1}[g_{9/2}]^2$ SD configuration shown in Fig. 4(c) is not a likely candidate for the observed band. The Q_t of

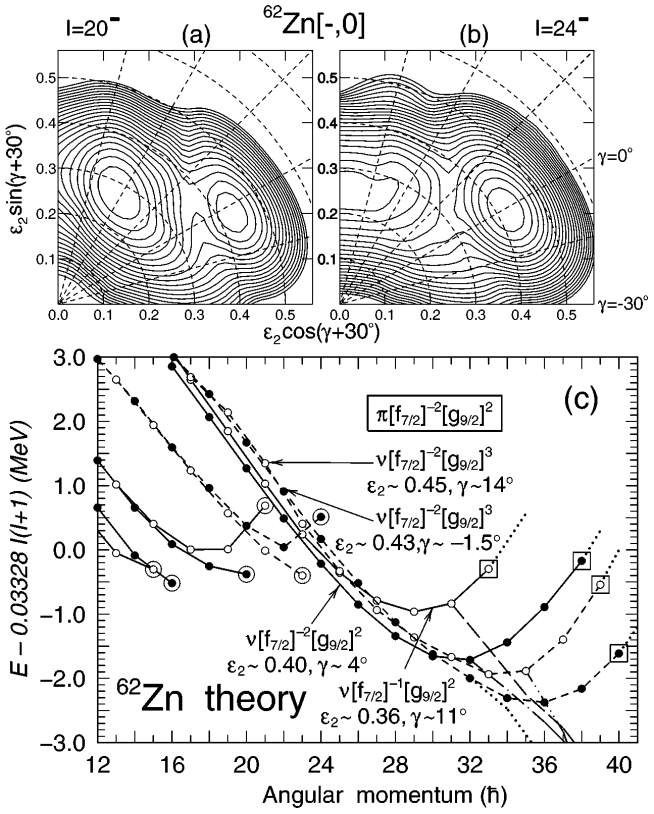

FIG. 4. Calculated high-spin properties of ^{62}Zn. Potential energy surfaces are shown for (a) $I^\pi = 20^-$ and (b) $I^\pi = 24^-$. Equipotential lines separated by 0.25 MeV are shown up to 5.5 MeV above the minima. (c) Energies of favored collective configurations relative to an $I(I+1)$ reference plotted versus spin. The SD configurations are labeled by their neutron and proton $f_{7/2}$ holes and $g_{9/2}$ particles and by their equilibrium deformations at $I \approx 22\hbar$. Solid (dashed) lines represent positive (negative) parity, and closed (open) symbols denote signature $\alpha = 0$ ($\alpha = +1$). Terminating ND states are encircled. For $I > 30\hbar$ the yrast lines for different combinations of parity and signature are shown by lines of different type without symbols. The states corresponding to the "maximum spin" extracted from the low-spin SD configurations are indicated by large open squares. Note that these states are collective and that the SD bands can be extended to higher spins, as indicated by the dotted lines.

2.1–1.2 e b calculated for this band is outside of the experimental uncertainty on the measured value, and the absence of the signature-partner band that should be observed with a single signature-degenerate $f_{7/2}$ hole also argues strongly against this configuration. It is expected that future experiments in this mass region will establish links between SD bands and ND states. The definite configuration assignments resulting from such links will provide important information on the, as yet unknown, single-particle energies at large deformation in this mass region. We also note that the states corresponding to the "maximum spin" extracted from the low-spin SD configurations [large open squares in Fig. 4(c)] occur at spins only slightly higher than observed in this experiment. Although these states are collective and the SD bands do not terminate in the usual sense, their properties in the $I = 30\hbar - 40\hbar$ range are strongly affected by the limited spin content of their single-particle configurations.

In summary, we have observed a cascade of six γ rays in ^{62}Zn that forms a rotational band over an estimated spin range of $I = 18\hbar - 30\hbar$. The scaled $J^{(2)}$ moment of inertia of this band is comparable to those of SD bands in other mass regions, and the measured quadrupole deformation of $\beta_2 = 0.45^{+0.10}_{-0.07}$ is in excellent agreement with theoretical calculations which indicate that SD bands with $\beta_2 = 0.41 - 0.49$ become yrast in ^{62}Zn for spins $I \geq 24\hbar$. These results establish a new region of superdeformation in nuclei with neutron and proton numbers $N, Z \approx 30 - 32$. A systematic study of SD bands in this mass region is clearly required to define the limits of this newest region of superdeformation and to extract detailed information about the single-particle energies at large deformation for these light nuclei.

This work has been partially funded by the Natural Sciences and Engineering Research Council of Canada, the U.S. D.O.E. under Contracts No. DE-AC05-96OR22464 and No. DE-AC03-76SF00098 and Grants No. DE-FG05-88ER40406 and No. DE-FG05-93ER40770, the German BMBF under Contracts No. 06-OK-668 and No. 06-LM-868, the Swedish Natural Science Research Council, and the Royal Swedish Academy of Sciences.

*Permanent address: Nuclear Research Center, Latvian Academy of Sciences, LV-2169 Salaspils, Latvia.

[1] P. J. Twin *et al.*, Phys. Rev. Lett. **57**, 811 (1986).
[2] X.-L. Han and C.-L. Wu, At. Data Nucl. Data Tables **63**, 117 (1996).
[3] R. K. Sheline, I. Ragnarsson, and S. G. Nilsson, Phys. Lett. **41B**, 115 (1972).
[4] J. Dudek *et al.*, Phys. Rev. Lett. **59**, 1405 (1987).
[5] I. Ragnarsson, in *Proceedings of the Workshop on the Science of Intense Radioactive Ion Beams*, edited by J. B. McClelland and D. J. Vieira (Los Alamos National Laboratory Report No. LA-11964-C, 1990), p. 199.
[6] D. J. Dean, in *Proceedings of the Conference on Nuclear Structure at the Limits* (Argonne National Laboratory Report No. ANL/PHY-97/1, 1997), p. 232.
[7] K. Nichols and R. A. Sorensen, Nucl. Phys. **A309**, 45 (1978).
[8] E. M. Müller *et al.*, Nucl. Phys. **A383**, 233 (1982).
[9] A. V. Afanasjev and I. Ragnarsson, Nucl. Phys. **A608**, 176 (1996).
[10] I.-Y. Lee, Nucl. Phys. **A520**, 641c (1990).
[11] D. G. Sarantites *et al.*, Nucl. Instrum. Methods Phys. Res., Sect. A **381**, 418 (1996).
[12] M. Devlin *et al.*, Nucl. Instrum. Methods Phys. Res., Sect. A **383**, 506 (1996).
[13] C. E. Svensson *et al.*, in *Proceedings of the Conference on Nuclear Structure at the Limits* (Argonne National Laboratory Report No. ANL/PHY-97/1, 1997), p. 209; Nucl. Instrum. Methods Phys. Res., Sect. A (to be published).
[14] C. E. Svensson *et al.* (to be published).
[15] A. Lopez-Martens *et al.*, Phys. Rev. Lett. **77**, 1707 (1996).
[16] D. P. Balamuth, T. Chapuran, and J. W. Arrison, Nucl. Instrum. Methods Phys. Res., Sect. A **275**, 315 (1989).
[17] D. F. Winchell *et al.*, Phys. Lett. B **289**, 267 (1992).
[18] B. Cederwall *et al.*, Nucl. Instrum. Methods Phys. Res., Sect. A **354**, 591 (1995).
[19] L. C. Northcliffe and R. F. Schilling, Nucl. Data Tables A **7**, 233 (1970).
[20] J. F. Ziegler and W. K. Chu, At. Data Nucl. Data Tables **13**, 463 (1974).
[21] S. H. Sie *et al.*, Nucl. Phys. **A291**, 443 (1977).
[22] H. Savajols *et al.*, Phys. Rev. Lett. **76**, 4480 (1996).
[23] T. Bengtsson and I. Ragnarsson, Nucl. Phys. **A436**, 14 (1985).
[24] A. V. Afanasjev and I. Ragnarsson, Nucl. Phys. **A591**, 387 (1995).